

Measuring CP Violation in $h \rightarrow \tau^+\tau^-$ at Colliders

Roni Harnik,¹ Adam Martin,^{2,3} Takemichi Okui,⁴ Reinard Primulando,⁵ and Felix Yu¹

¹*Theoretical Physics Department, Fermilab, P.O. Box 500, Batavia, IL 60510, USA*

²*Department of Physics, University of Notre Dame, Notre Dame, IN 46556, USA*

³*PH-TH Department, CERN, CH-1211 Geneva 23, Switzerland*

⁴*Department of Physics, Florida State University, Tallahassee, Florida 32306-4350, USA*

⁵*Department of Physics and Astronomy, Johns Hopkins University, Baltimore, MD 21218, USA*

We investigate the LHC and Higgs Factory prospects for measuring the CP phase in the Higgs- $\tau\tau$ coupling. Currently this phase can be anywhere between 0° (CP even) and 90° (CP odd). A new, ideal observable is identified from an analytic calculation for the $\tau^\pm \rightarrow \rho^\pm \nu \rightarrow \pi^\pm \pi^0 \nu$ channel. It is demonstrated to have promising sensitivity at the LHC and superior sensitivity at the ILC compared to previous proposals. Our observable requires the reconstruction of the internal substructure of decaying taus but does not rely on measuring the impact parameter of tau decays. It is the first proposal for such a measurement at the LHC. For the 14 TeV LHC, we estimate that about 1 ab^{-1} data can discriminate CP -even versus CP -odd at the 5σ level. With 3 ab^{-1} , the CP phase should be measurable to an accuracy of $\sim 11^\circ$. At an e^+e^- Higgs Factory, we project that a 250 GeV run with 1 ab^{-1} luminosity can measure the phase to $\sim 4.4^\circ$ accuracy.

I. INTRODUCTION

The discovery of the Higgs boson [1, 2] has opened a new opportunity in the search for physics beyond the SM. The SM predicts all couplings of the Higgs to SM particles completely, and a measured significant deviation of Higgs couplings from the SM prediction will be a clear signal of new physics. The most straightforward tests at the moment are comparisons of the Higgs production rates times branching ratios to the SM prediction in a variety of final states. Thus far, such global fits roughly agree with a SM Higgs [3, 4].

We can go further by testing the CP properties of Higgs couplings. This test has already been done for the coupling of the Higgs to electroweak gauge bosons [5, 6]. In the SM, the Higgs couples to the Z boson as a scalar, $hZ_\mu Z^\mu$. In general, a Higgs-like state could couple to Z bosons as a pseudoscalar, $hZ_{\mu\nu}\tilde{Z}^{\mu\nu}$, or with any linear combination of scalar and pseudoscalar couplings, which would imply CP violation. In the fully leptonic channel for $h \rightarrow ZZ^*$, the azimuthal angle between the decay planes of the two Z bosons is sensitive to the Z polarizations, which in turn is sensitive to the CP structure of the Higgs couplings [7]. Current data disfavors a pure pseudoscalar coupling at $99.84\% = 3.3 \sigma$ and 99.6% (97.8%) confidence level using CL_S statistics at CMS [5] and ATLAS MELA (ATLAS BDT) [6], respectively.

In models where the SM is augmented by heavy new physics, this result is unsurprising. Of the two possible interactions mentioned above, the scalar interaction is renormalizable, while the pseudoscalar interaction arises from a dimension six operator. The pseudoscalar coupling is thus expected to be subdominant in Higgs decays and corresponding CP violating effects will be small. While current results favor a pure scalar coupling in the Higgs couplings to weak gauge bosons, searches for CP violation in fermionic decays of the Higgs are still highly motivated. Such modified couplings can arise from a dif-

ferent source which, in particular, can give a pseudoscalar interaction comparable to a scalar, unlike the Higgs- W/Z couplings.

In this paper we investigate how the CP structure of the coupling of the Higgs to tau leptons can be probed at present and future colliders. The Higgs coupling to any fermion generally consists of a CP even and a CP odd term,

$$\mathcal{L}_{hff} \propto h\bar{f}(\cos \Delta + i\gamma_5 \sin \Delta)f. \quad (1)$$

Measuring this CP phase Δ requires knowledge of the spins of the $f\bar{f}$ state. Tau decays are complex enough to retain non-trivial information about the direction of the tau spin, yet clean enough that the spin information is not washed out by hadronization effects as it is for b -quark decays [8]. Since the Higgs branching fraction to $\tau^+\tau^-$ is substantial in the SM ($\sim 6.15\%$ for $m_h = 126$ GeV), the $\tau^+\tau^-$ decay channel is the best of a limited set of opportunities for CP violation searches in Higgs couplings to fermions.¹ In addition, a pseudoscalar-like coupling of the Higgs to taus can conceivably compete with the small tau Yukawa coupling, and so CP violating effects can be sizable. Currently, the only direct bound on the Higgs-tau coupling is on the net signal strength in $h \rightarrow \tau^+\tau^-$ channels: $\hat{\mu} = 1.1 \pm 0.4$ [11]. In this paper, we will maintain $\hat{\mu} = 1$ and modify only Δ , so this constraint does not apply.

We focus on the specific tau decay channel $\tau^\pm \rightarrow \rho^\pm \nu$ with $\rho^\pm \rightarrow \pi^\pm \pi^0$. This is the most common tau decay sub-channel, with a branching fraction of $\sim 25\%$. Moreover, the angular distributions of the tau decay products and subsequent rho decay products are correlated with the original direction of the tau spin, as we will see in section III A. The relative azimuthal orientation of the

¹ For opportunities in other channels see [9, 10].

two hadronic taus, Θ , which we will define precisely in section III C, contains information about the CP properties of the Higgs coupling to taus. In particular, the CP phase Δ in the Higgs couplings may be read off directly from the Θ distribution. The differential cross section is shown analytically in sections III B and C to have the form $c - A \cos(\Theta - 2\Delta)$, and Δ may be measured by finding the minimum of the distribution (as exemplified in figure 2). The dominant background for $h \rightarrow \tau\tau$ events at the LHC is $Z \rightarrow \tau\tau$, which produces a flat Θ distribution.

The ability to distinguish scalar versus pseudoscalar Higgs couplings in the tau channel has been discussed in [12–22]. Our work quantitatively improves on these results: our Θ variable is demonstrably more sensitive to the CP phase of the Higgs coupling to taus compared to earlier proposed observables, and our simulation results for the ILC indicate a corresponding increase in sensitivity compared to earlier results. This work is also a qualitative step forward in that we propose a strategy to do this measurement at the LHC. Previous studies relied on resolving a displaced vertex in τ decays which is challenging. We show that our observable retains sensitivity without this.

It should be stressed that in order to reconstruct the angle Θ , full knowledge of all four-momenta components in the event is needed, including those of the two neutrinos. We will discuss the challenges that this presents and how they may be addressed. In the context of a Higgs factory (ILC), $h \rightarrow \tau^+\tau^- \rightarrow \rho^+\rho^-\nu\bar{\nu}$ events may be fully reconstructed up to a two-fold ambiguity. Furthermore, a favorable signal to background ratio makes our measurement straightforward. At a hadron collider, however, some approximations are needed for the neutrino four-momenta. Employing the collinear approximation [23], we show that the amplitude of the angular structure in Θ is only reduced by an order one factor for $h \rightarrow \tau\tau$ signal events. The challenge for the LHC is thus to increase the signal to background ratio as much as possible in order to produce a statistically significant result. In addition, an improvement over the collinear approximation would make a positive impact on the resulting sensitivity to Δ .

Our net result is that, using the Θ variable, a measurement of Δ with an accuracy of 4.4° is possible for a $\sqrt{s} = 250$ GeV e^+e^- collider, assuming 1 ab^{-1} of luminosity (without incorporating detector effects, which are expected to be negligibly small). This number should be compared with the result of Ref. [18], which quotes an accuracy of measuring Δ to 6° using the same amount of luminosity but for $\sqrt{s} = 350$ GeV and $m_h = 120$ GeV. We also provide the first estimates for sensitivity to Δ at the LHC. Without incorporating detector effects or pileup, we find an ideal measurement of Δ to an accuracy of 11.5° is possible with 3 ab^{-1} of $\sqrt{s} = 14$ TeV LHC data for a τ -tagging efficiency of 50%. Improving the efficiency from 50% to 70% could lead to an accuracy of 8.0° using the same LHC luminosity.

This paper is organized as follows. In section II we add CP violation to the Higgs coupling to tau leptons. In section III we introduce our observable, first in a heuristic analysis that follows every step of the decay, and then rigorously, using the analytic form of the full $1 \rightarrow 6$ differential cross section. We present the results of our collider analyses in section IV. We first present the relevant distributions using Monte Carlo truth information, then reevaluate in a Higgs factory setup, where a twofold ambiguity needs to be considered, and finally consider an LHC setting using the collinear approximation. We conclude in section V. A weakly-coupled renormalizable model giving rise to CP violation in the Higgs coupling to taus is presented in appendix A.

II. A CP -VIOLATING $h\tau\bar{\tau}$ COUPLING

In our study of the CP nature of $h \rightarrow \tau^+\tau^-$, we use the following phenomenological Lagrangian:

$$\begin{aligned} \mathcal{L}_{\text{pheno}} \supset & -m_\tau \bar{\tau}\tau - \frac{y_\tau}{\sqrt{2}} h \bar{\tau} (\cos \Delta + i\gamma_5 \sin \Delta) \tau \\ & = -m_\tau \bar{\tau}\tau - \frac{y_\tau}{\sqrt{2}} h (\tau_L^\dagger (\cos \Delta + i \sin \Delta) \tau_R \\ & \quad + \text{c.c.}), \end{aligned} \quad (2)$$

where τ and h are the physical tau lepton and Higgs boson in the mass basis, respectively, y_τ is a real parameter parametrizing the magnitude of the $h\tau\bar{\tau}$ coupling, and, most importantly, $\Delta \in (-\pi/2, \pi/2]$ is an angle describing the CP nature of the $h\tau\bar{\tau}$ coupling.² The CP -even and CP -odd cases correspond to $\Delta = 0$ and $\Delta = \pi/2$, respectively, while $\Delta = \pm\pi/4$ describe maximally CP -violating cases. The SM corresponds to a special case, $y_\tau = y_\tau^{\text{SM}} \equiv m_\tau/v$ with $\Delta = 0$. We will refer to “ $\cos \Delta + i \sin \Delta$ ” as a “ CP -violating $h\tau\bar{\tau}$ coupling”, even though it includes the CP -conserving limits of $\Delta = 0$ and $\pi/2$. In this work, we focus on the effects of Δ , so we will take $y_\tau = y_\tau^{\text{SM}}$ while treating Δ as a free parameter.

The simplest fully gauge-invariant operator that results in the CP -violating $h\tau\bar{\tau}$ coupling (2) upon electroweak symmetry breaking is given by

$$\mathcal{L}_{\text{eff}} \supset -\left(\alpha + \beta \frac{H^\dagger H}{\Lambda^2}\right) H \ell_{3L}^\dagger \tau_R + \text{c.c.}, \quad (3)$$

where α and β are *complex* dimensionless parameters, and Λ is a mass scale taken to be real and positive without loss of generality. To relate the parameters of $\mathcal{L}_{\text{pheno}}$ and \mathcal{L}_{eff} , we substitute $H = (0, v + h/\sqrt{2})^T$ in (3), which

² The angle Δ can, in fact, take the full range of $(-\pi, \pi]$. However our technique is not sensitive to a multiplication of the tau Yukawa by -1 and so it is sufficient to consider half of this range. Resolving this ambiguity would require measuring the interference of Higgs with background, which is a tiny effect.

yields

$$\mathcal{L}_{\text{eff}} \supset -\left(\alpha + \beta \frac{v^2}{\Lambda^2}\right) v \tau_L^\dagger \tau_R - \left(\alpha + 3\beta \frac{v^2}{\Lambda^2}\right) \frac{h}{\sqrt{2}} \tau_L^\dagger \tau_R + \text{c.c.}, \quad (4)$$

from which we identify

$$\alpha + \beta \frac{v^2}{\Lambda^2} = y_\tau^{\text{SM}} > 0, \quad (5)$$

and we have taken y_τ^{SM} to be real and positive (hence $m_\tau \equiv y_\tau^{\text{SM}} v$ is real and positive) without loss of generality after suitable redefinition of the phase of τ_R . With this phase convention, the $h\tau\bar{\tau}$ coupling in (2) is generally complex:

$$y_\tau (\cos \Delta + i \sin \Delta) = \alpha + 3\beta \frac{v^2}{\Lambda^2} = y_\tau^{\text{SM}} + 2\beta \frac{v^2}{\Lambda^2}. \quad (6)$$

Since $y_\tau^{\text{SM}} \sim 10^{-2}$, new physics at the TeV scale ($\Lambda \sim 10v$) with $\mathcal{O}(1)$ couplings ($|\beta| \sim 1$) can give rise to Δ anywhere in the full range $(-\pi/2, \pi/2]$.³ This is in stark contrast to the case of a CP -odd/violating Higgs coupling to Z bosons, where TeV-scale new physics is expected to give only small corrections to the SM CP -even coupling.

III. THE OBSERVABLE

To probe the CP -violating $h\tau\bar{\tau}$ coupling in (2), we will study the following decay process:

$$\begin{aligned} h &\longrightarrow \tau^- \tau^+ \\ &\longrightarrow \rho^- \nu_\tau \rho^+ \bar{\nu}_\tau \\ &\longrightarrow \pi^- \pi^0 \nu_\tau \pi^+ \pi^0 \bar{\nu}_\tau. \end{aligned} \quad (7)$$

There are several good reasons to choose this decay chain. First, to minimize the loss of kinematic information due to neutrinos, we want both τ^- and τ^+ to decay hadronically. Second, of the hadronic decay modes, we choose $\tau \rightarrow \rho\nu$, since the subsequent decay, $\rho^\pm \rightarrow \pi^\pm \pi^0$, can be reconstructed at a collider. Third, $\tau \rightarrow \rho\nu$ has the largest branching fraction of any individual tau decay mode, $\sim 25\%$, and the following step, $\rho \rightarrow \pi\pi$, occurs with a nearly 100% probability. Finally, the ρ width is sufficiently narrow that it is well justified to consider it on-shell, which makes the process in (7) an analytically tractable sequence of 2-body decays.

We begin with a heuristic look at the process in (7) to develop a rough idea of how it can probe the CP -violating $h\tau\tau$ coupling (2). In particular, the highlights of qualitative points to be made in sections III A 1, A 2 and A 3 are:

- 1: Measuring τ helicities cannot determine the CP phase, but the τ polarizations in directions *perpendicular* to the τ momenta can.
- 2: In the tau rest frame the ρ is predominantly longitudinal and is polarized roughly in the direction of the τ polarization.
- 3: The difference between the charged and neutral pion 3-momenta, $\vec{p}_{\pi^\pm} - \vec{p}_{\pi^0}$, is roughly parallel to the respective ρ^\pm polarization.

Therefore, the CP nature of $h \rightarrow \tau\tau$ must be encoded in the orientation of “ $\vec{p}_{\pi^\pm} - \vec{p}_{\pi^0}$ ” in the plane perpendicular to the τ^\pm momenta in the Higgs rest frame. A precise form of “ $\vec{p}_{\pi^\pm} - \vec{p}_{\pi^0}$ ” as well as the best observable to measure the CP phase Δ will be identified in sections III B and C by analytically computing the full matrix element for the sequence of two-body decays in process (7).

A. A heuristic analysis

1. $h \rightarrow \tau^- \tau^+$

The most general form of the amplitude for the decay $h \rightarrow \tau^- \tau^+$ is given by

$$\mathcal{M}_{h \rightarrow \tau\tau} \propto \sum_{s,s'} \chi_{s,s'} \bar{u}_{\tau^-}^s (\cos \Delta + i\gamma_5 \sin \Delta) v_{\tau^+}^{s'}, \quad (8)$$

where $\chi_{s,s'}$ is the probability amplitude of τ^- and τ^+ having helicities $s/2$ and $s'/2$, respectively. Lorentz invariance dictates that the proportionality factor omitted in (8) has no momentum dependence.

In the Higgs rest frame, the amplitude (8) takes the form

$$\mathcal{M}_{h \rightarrow \tau\tau} \propto |\vec{p}_{\tau^-}| \chi_0^1 \cos \Delta - i E_{\tau^-} \chi_0^0 \sin \Delta, \quad (9)$$

where \vec{p}_{τ^-} and E_{τ^-} are the τ^- momentum and energy in this frame, while χ_m^j is the linear combination of $\chi_{s,s'}$ with angular momentum (j, m) . In particular,

$$\chi_0^1 = \frac{\chi_{1,1} + \chi_{-1,-1}}{\sqrt{2}}, \quad \chi_0^0 = \frac{\chi_{1,1} - \chi_{-1,-1}}{\sqrt{2}}. \quad (10)$$

The amplitude in (9) shows that the CP -even contribution ($\propto \cos \Delta$) is a spin triplet in a p -wave, while the CP -odd contribution ($\propto \sin \Delta$) is a spin singlet in an s -wave. This can be understood as a consequence of angular momentum conservation and Fermi statistics, with the additional fact that a fermion-anti-fermion pair has an odd intrinsic parity.

³ An “existence proof” of such new physics in terms of a weakly-coupled renormalizable theory is given in appendix A.

To measure Δ , it is necessary to keep the $\tau^-\tau^+$ pair in the above superpositions of $\chi_{1,1}$ and $\chi_{-1,-1}$, without projecting the polarizations onto the helicity eigenstates. From (9) and (10), we see that the coefficients of $\chi_{1,1}$ and $\chi_{-1,-1}$ are the complex conjugates of each other, which implies that, regardless of Δ , the probability for both τ^- and τ^+ to be right-handed is always equal to that for both to be left-handed. Therefore, to distinguish the two linear combinations in (10), we must measure the polarizations in the directions *perpendicular* to the momenta, as mentioned in item 1 above.

2. $\tau^- \rightarrow \rho^- \nu_\tau$

Assuming the SM weak interactions for the τ and ν_τ , the most general form of the amplitude for $\tau^- \rightarrow \rho^- \nu_\tau$ is given by

$$\mathcal{M}_{\tau \rightarrow \rho \nu} \propto (\epsilon_{\rho^-}^*)_\mu \bar{u}_{\nu_\tau} \gamma^\mu P_L u_{\tau^-}, \quad (11)$$

with $P_L \equiv (1 - \gamma_5)/2$. Again, Lorentz invariance dictates that the proportionality factor omitted in (11) has no momentum dependence.

In the τ^- rest frame, the amplitude (11) has the form

$$\mathcal{M}_{\tau \rightarrow \rho \nu} \propto \epsilon_{\rho^-}^* \cdot \left(\varepsilon_{-1} \sin \frac{\theta}{2} - \varepsilon_0 \frac{m_\tau}{\sqrt{2} m_\rho} \cos \frac{\theta}{2} \right), \quad (12)$$

where $\theta \in [0, \pi]$ is the angle between the ρ^- momentum and the τ^- polarization in this frame, and ε_{-1}^μ , ε_0^μ , and ε_1^μ are the polarization vectors for the left-handed, longitudinal, and right-handed polarizations of the ρ^- , respectively. Since $m_\tau^2/(2m_\rho^2) \sim 3$, the amplitude (12) is dominated by the second term, roughly speaking. Thus, we are led to the picture described in the item 2 above, namely, the ρ^- is predominantly longitudinal ($\epsilon_{\rho^-} \sim \varepsilon_0$) and mostly emitted in the direction of the τ^- polarization ($\theta \sim 0$).

3. $\rho^- \rightarrow \pi^- \pi^0$

The most general form of the amplitude for $\rho^- \rightarrow \pi^- \pi^0$ is given by

$$\mathcal{M}_{\rho \rightarrow \pi \pi} \propto \epsilon_{\rho^-} \cdot (p_{\pi^-} - p_{\pi^0}). \quad (13)$$

The other linear combination, $p_{\pi^-} + p_{\pi^0}$, cannot appear here because $\epsilon_{\rho^-} \cdot (p_{\pi^-} + p_{\pi^0}) = \epsilon_{\rho^-} \cdot p_{\rho^-} = 0$. Again, the proportionality factor omitted in (13) cannot have any momentum dependence by Lorentz invariance.

Boosting the longitudinal ρ^- to its rest frame, and neglecting the $\pi^\pm - \pi^0$ mass difference, the amplitude (13) takes the form

$$\mathcal{M}_{\rho \rightarrow \pi \pi} \propto |\vec{p}_{\pi^-} - \vec{p}_{\pi^0}| \cos \psi, \quad (14)$$

where ψ is the angle between the original ρ^- polarization and the vector $\vec{p}_{\pi^-} - \vec{p}_{\pi^0}$ in the rest frame. Therefore,

the momentum difference, $\vec{p}_{\pi^-} - \vec{p}_{\pi^0}$, is roughly (anti-)parallel ($\psi \sim 0$ or π) to the original ρ^- polarization, as we described in the item 3 above.

B. The “electric” and “magnetic” variables

We now analytically compute the full matrix element for the process (7) to identify the observable that is most sensitive to the CP phase Δ . Combining the amplitudes (8), (11) and (13), the full amplitude for the process (7) at tree level is given by

$$\begin{aligned} \mathcal{M}_{\text{full}} \propto & \bar{u}_{\nu^-} (\not{p}_{\pi^-} - \not{p}_{\pi^0}) P_L (\not{p}_{\tau^-} + m_\tau) \\ & \times (\cos \Delta + i\gamma_5 \sin \Delta) \\ & \times (-\not{p}_{\tau^+} + m_\tau) (\not{p}_{\pi^+} - \not{p}_{\pi^0}) P_L v_{\nu^+}, \end{aligned} \quad (15)$$

where $\pi^{0\pm}$ refers to the π^0 coming from the ρ^\pm decay, respectively, and we have denoted ν_τ and $\bar{\nu}_\tau$ as ν^- and ν^+ , respectively. The following approximations have been made above:

- We neglected the diagram in which the two π^0 are exchanged, assuming that we can identify $\pi^{0\pm}$ by looking for a π^0 flying near π^\pm , respectively. As the taus from $h \rightarrow \tau^+\tau^-$ are highly boosted and back-to-back in the Higgs rest frame, this should be an excellent approximation.
- All intermediate particles are assumed to be on-shell, so the denominators of their propagators have been dropped in (15), as they are just momentum-independent constants $\sim i m \Gamma$.
- We neglect $m_{\pi^\pm} - m_{\pi^0}$ throughout the paper. A convenient consequence of this (very good) approximation is that the $\rho\pi\pi$ amplitude in (13) effectively satisfies a “Ward identity”, *i.e.*, it vanishes upon replacing ϵ_{ρ^-} with p_{ρ^-} :

$$p_{\rho^-} \cdot (p_{\pi^-} - p_{\pi^0}) = m_{\pi^\pm}^2 - m_{\pi^0}^2 = 0. \quad (16)$$

This is why we have dropped the $p_\mu p_\nu / m_\rho^2$ term of the ρ^\pm propagators in (15).

Carefully keeping the combinations $p_{\pi^\pm} - p_{\pi^0}$ intact as suggested by the heuristic analysis of section III A, the amplitude (15) can be rewritten as

$$\mathcal{M}_{\text{full}} \propto \bar{u}_{\nu^-} \not{q}_- (e^{i\Delta} \not{p}_{\tau^-} - e^{-i\Delta} \not{p}_{\tau^+}) \not{q}_+ P_L v_{\nu^+}, \quad (17)$$

where

$$q_\pm \equiv p_{\pi^\pm} - p_{\pi^0}. \quad (18)$$

Taking $\{p_{\tau^\pm}, q_\pm, p_{\nu^\pm}\}$ as the set of independent variables (subject to the constraint $(p_{\tau^+} + p_{\tau^-})^2 = m_h^2$), let us analyze how the physics depends on these momenta. First, in the square of the amplitude (17), the variables q_\pm and p_{ν^\pm} will only enter via the products $\not{q}_+ \not{p}_{\nu^+} \not{q}_+$ and

$\not{q}_- \not{p}_\nu - \not{q}_-$. These combinations can be further simplified as

$$\not{q}_\pm \not{p}_\nu \not{q}_\pm = (m_\tau^2 + m_\rho^2) \not{k}_\pm, \quad (19)$$

where

$$k_\pm^\mu \equiv y_\pm q_\pm^\mu + r p_{\nu\pm}^\mu \quad (20)$$

with⁴

$$y_\pm \equiv \frac{2q_\pm \cdot p_{\tau\pm}}{m_\tau^2 + m_\rho^2} = \frac{q_\pm \cdot p_{\tau\pm}}{p_{\rho\pm} \cdot p_{\tau\pm}}, \quad (21)$$

$$r \equiv \frac{m_\rho^2 - 4m_\pi^2}{m_\tau^2 + m_\rho^2} \approx 0.14. \quad (22)$$

In terms of k_\pm and $p_{\tau\pm}$, the square of the amplitude in (17) only involves the traces over four γ matrices, and an elementary computation gives

$$|\mathcal{M}|^2 \propto P_{\Delta,S} + P_{\Delta,\mathcal{S}} + P_{\Delta,S} + P_{\Delta,S}^*, \quad (23)$$

where

$$P_{\Delta,S} \equiv 2[(k_- \cdot p_{\tau-})(p_{\tau-} \cdot k_+) + (k_+ \cdot p_{\tau+})(p_{\tau+} \cdot k_-) - m_\tau^2 (k_- \cdot k_+)], \quad (24)$$

$$P_{\Delta,\mathcal{S}} \equiv -2 \cos(2\Delta) (k_- \cdot p_{\tau-})(k_+ \cdot p_{\tau+}), \quad (25)$$

$$P_{\Delta,S} \equiv -e^{2i\Delta} [(k_- \cdot p_{\tau+})(k_+ \cdot p_{\tau-}) - (p_{\tau-} \cdot p_{\tau+})(k_- \cdot k_+) - i\epsilon_{\mu\nu\rho\sigma} k_-^\mu p_{\tau-}^\nu k_+^\rho p_{\tau+}^\sigma]. \quad (26)$$

Here, $P_{\Delta,S}$ is the interesting contribution that depends on both Δ and the τ^\pm spins. On the other hand, $P_{\Delta,\mathcal{S}}$ is an uninteresting piece since it is independent of Δ . (It is sensitive to the τ^\pm spins, *i.e.*, the relative orientation of the τ^+ and τ^- subsystems, as it involves scalar products like $k_- \cdot k_+$). Lastly, $P_{\Delta,\mathcal{S}}$ does depend on Δ but is insensitive to the spins, as it only involves $k_+ \cdot p_{\tau+}$ and $k_- \cdot p_{\tau-}$, which are just scalar quantities of the τ^+ and τ^- subsystems alone.

We therefore focus on $P_{\Delta,S}$. To reveal how it depends on the relative orientations of the τ^\pm systems to each other, observe that $P_{\Delta,S}$ is antisymmetric under $k_\pm \leftrightarrow p_{\tau\pm}$. This suggests that k_\pm and $p_{\tau\pm}$ should be combined into two antisymmetric tensors $F_\pm^{\mu\nu}$, one for each τ^\pm system:

$$F_\pm^{\mu\nu} \equiv k_\pm^\mu p_{\tau\pm}^\nu - k_\pm^\nu p_{\tau\pm}^\mu = -F_\pm^{\nu\mu}. \quad (27)$$

In terms of these, $P_{\Delta,S}$ takes an elegant form:

$$P_{\Delta,S} = e^{2i\Delta} \left(\frac{1}{2} F_{-\mu\nu} F_+^{\mu\nu} + \frac{i}{4} \epsilon_{\mu\nu\rho\sigma} F_-^{\mu\nu} F_+^{\rho\sigma} \right). \quad (28)$$

Moreover, the fact that $F_\pm^{\mu\nu}$ are antisymmetric 2nd-rank tensors suggests that the physics is clearest in terms of their ‘‘electric’’ and ‘‘magnetic’’ components:

$$E_\pm^i \equiv F_\pm^{i0}, \quad B_\pm^i \equiv -\frac{1}{2} \epsilon^{ijk} F_{\pm jk}. \quad (29)$$

Indeed, $P_{\Delta,S}$ then simplifies into just one term:

$$P_{\Delta,S} = -e^{2i\Delta} [(\vec{E}_- + i\vec{B}_-) \cdot (\vec{E}_+ + i\vec{B}_+)]. \quad (30)$$

We will now develop intuition for \vec{E}_\pm and \vec{B}_\pm . First, from (29), we have

$$\vec{B}_\pm = \vec{p}_{\tau\pm} \times \vec{k}_\pm = \vec{v}_{\tau\pm} \times \vec{E}_\pm, \quad (31)$$

where $\vec{v}_{\tau\pm} \equiv \vec{p}_{\tau\pm}/p_{\tau\pm}^0$ is the 3-velocity of the τ^\pm . Thus, $\vec{B}_\pm = 0$ in the rest frame of each τ^\pm , respectively, while in all other frames \vec{B}_\pm are perpendicular to both \vec{E}_\pm and $\vec{p}_{\tau\pm}$. Moreover, in the boosted τ^\pm limit ($|\vec{v}_{\tau\pm}| \rightarrow 1$), we have $|\vec{B}_\pm| = |\vec{E}_\pm|$.

Second, from (29), \vec{E}_\pm is given by

$$\vec{E}_\pm = p_{\tau\pm}^0 \vec{k}_\pm - k_\pm^0 \vec{p}_{\tau\pm}. \quad (32)$$

Clearly, \vec{E}_\pm takes the simplest form in the τ^\pm rest frame since then $\vec{p}_{\tau\pm}$ in the second term vanishes. Let us use $|_0$ to indicate the quantities evaluated in the respective τ^\pm rest frames. Then, combining (20) and (32) in the τ^\pm rest frames, we have

$$\begin{aligned} \vec{E}_\pm|_0 &= m_\tau \vec{k}_\pm|_0 \\ &= m_\tau [(y_\pm - r) \vec{p}_{\tau\pm}|_0 - (y_\pm + r) \vec{p}_{\tau^0\pm}|_0], \end{aligned} \quad (33)$$

where we have used $\vec{p}_{\nu\pm}|_0 = -\vec{p}_{\tau\pm}|_0 - \vec{p}_{\tau^0\pm}|_0$. Therefore, in an arbitrary frame with a τ^\pm velocity $\vec{v}_{\tau\pm}$, we have

$$\begin{aligned} \vec{E}_\pm^\parallel &= \vec{E}_\pm^\parallel|_0, \\ \vec{E}_\pm^\perp &= \gamma_\pm [\vec{E}_\pm|_0 - \vec{v}_{\tau\pm} \times \vec{B}_\pm|_0]^\perp = \frac{E_{\tau\pm}}{m_\tau} \vec{E}_\pm^\perp|_0, \end{aligned} \quad (34)$$

where \vec{E}_\pm^\parallel and \vec{E}_\pm^\perp are the components of \vec{E}_\pm parallel and perpendicular to $\vec{v}_{\tau\pm}$, respectively, while $\gamma_\pm \equiv (1 - |\vec{v}_{\tau\pm}|^2)^{-1/2} = E_{\tau\pm}/m_\tau$. An important implication of (34) is that, for a boosted τ^\pm ($E_{\tau\pm}/m_\tau \gg 1$), we get $|\vec{E}_\pm^\perp| \gg |\vec{E}_\pm^\parallel|$, so \vec{E}_\pm also becomes perpendicular to $\vec{v}_{\tau\pm}$. Thus, the relative magnitudes and orientations of \vec{E}_\pm , \vec{B}_\pm , and $\vec{v}_{\tau\pm}$ in the boosted τ^\pm limit are akin to those of electromagnetic waves.

To summarize, we write out \vec{E}_\pm and \vec{B}_\pm in the Higgs rest frame. Since the τ^\pm are highly boosted in this frame, we can neglect \vec{E}_\pm^\parallel . Then, combining (33) and (34) with $E_{\tau\pm} = m_h/2$, we get

$$\vec{E}_\pm = \frac{m_h}{2} [(y_\pm - r) \vec{p}_{\tau\pm}|_0 - (y_\pm + r) \vec{p}_{\tau^0\pm}|_0]^\perp, \quad (35)$$

⁴ $y_{+,-}$ are respectively equal to $y_{1,2}$ used in Refs. [15–18].

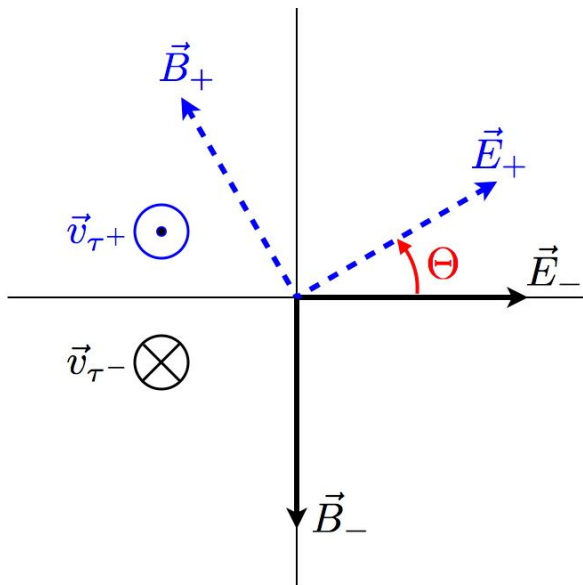


FIG. 1: The definition of our variable Θ , drawn in the Higgs rest frame with the τ^- and τ^+ going in and out of the page respectively. Note Θ is taken to be positive if \vec{E}_+ is on the upper-half plane, and negative otherwise, where \vec{E}_- is fixed to lie along the $+\hat{x}$ axis.

where $|_0$ on a vector indicates that the vector should be evaluated in the respective τ^\pm rest frame, while $^\perp$ denotes the components perpendicular to the respective τ^\pm velocity in the Higgs rest frame. Recall \vec{B}_\pm is given by (31).

C. The Θ angle

We are ready to evaluate $P_{\Delta,S}$ in the Higgs rest frame. In this frame, since \vec{v}_{τ^+} and \vec{v}_{τ^-} are back to back, the $\vec{E}_+-\vec{B}_+$ plane and the $\vec{E}_--\vec{B}_-$ plane are parallel to each other. Thus, we will superimpose them to make a single plane. In this combined plane, let \vec{E}_- and \vec{B}_- point to the right and downward, respectively. (See figure 1.) Then, we define Θ to be the angle of \vec{E}_+ with respect to \vec{E}_- , where $0 \leq \Theta \leq \pi$ if \vec{E}_+ is on the upper-half plane, while $-\pi < \Theta < 0$ if on the lower-half plane.⁵ That is,

$$\Theta = \text{sgn} \left[\vec{v}_{\tau^+} \cdot (\vec{E}_- \times \vec{E}_+) \right] \text{Arccos} \left[\frac{\vec{E}_+ \cdot \vec{E}_-}{|\vec{E}_+| |\vec{E}_-|} \right], \quad (36)$$

where Arccos takes values between 0 and $+\pi$. Then \vec{B}_+ makes an angle $\Theta + \pi/2$ with respect to \vec{E}_- . The magni-

⁵ In other words, Θ is the acoplanarity angle between the $\vec{E}_+-\vec{v}_{\tau^+}$ plane and $\vec{E}_--\vec{v}_{\tau^-}$ plane, where the orientation of the planes defined by the respective \vec{B}_\pm .

tudes of \vec{B}_\pm are the same as the respective \vec{E}_\pm . Putting everything together, the distribution (30) becomes

$$P_{\Delta,S} = -2e^{i(2\Delta-\Theta)} |\vec{E}_+| |\vec{E}_-|, \quad (37)$$

where \vec{E}_\pm are given by (35). The contributions that have been neglected to arrive at (37) from (26) are only $\mathcal{O}(m_\tau^2/m_h^2) \sim 0.01\%$.

IV. COLLIDER STUDIES

In this section we develop collider analyses aimed at reconstructing the Θ angle in (36). From (23) and (37), the matrix element squared for the $h \rightarrow \pi^+\pi^0\bar{\nu}\pi^-\pi^0\nu$ decay has a term proportional to $-\cos(\Theta - 2\Delta)$: the Θ distribution is thus sensitive to the CP phase Δ as its minimum is located at 2Δ . As before, we fix $y_\tau \equiv y_\tau^{\text{SM}}$ and therefore the only new parameter we introduce is Δ .

We implement the Δ phase in (2) and the effective vertices in (11) and (13) into a FeynRules v.1.6.0 [24] model. We then generate Monte Carlo events in MadGraph 5 [25] for $pp \rightarrow hj$ production at the LHC with $\sqrt{s} = 14$ TeV as well as $e^+e^- \rightarrow Zh$ production at the ILC with $\sqrt{s} = 250$ GeV: in either case, the Higgs decays via $h \rightarrow \pi^+\pi^0\bar{\nu}\pi^-\pi^0\nu$. In order to retain quantum interference effects, the full $2 \rightarrow 7$ body process is simulated. For the LHC study, we also generate a background sample of $pp \rightarrow Zj$ production with the subsequent decay $Z \rightarrow \pi^+\pi^0\bar{\nu}\pi^-\pi^0\nu$.

We will first study the effectiveness of the Θ distribution at truth level, assuming the neutrino momenta are known: this facilitates a comparison to the ϕ^* variable [15, 16], which was previously proposed for studying CP violation in the Higgs coupling to taus. After demonstrating the superior qualities of the Θ variable, we present a sensitivity study for reconstructing Θ at the ILC, where the neutrino four-momentum can be reconstructed up to a two-fold ambiguity. Finally, we turn to the LHC, where the neutrinos cannot be reconstructed and the irreducible Z background is significant. In this case, we find that using a collinear approximation [23] for the neutrino momenta in addition to the standard hard cuts for Higgs events still allows the Θ distribution to retain significant discrimination power between different underlying Δ signal models.

We do not include pileup or perform any detector simulation in this work, aside from implementing flat efficiencies for τ -tagging for the LHC study. Pileup effects are expected to complicate the primary vertex determination necessary for measuring charged pion tracks as well as contribute extra ambient radiation in the electromagnetic calorimeter (ECAL), making neutral pion momenta measurements more difficult. Furthermore, finite tracking and calorimeter resolutions are expected to smear the Θ distribution. In particular, the ability to distinguish between charged and neutral pion momenta when both pions are overlapping also could affect the Θ

measurement. Note, however, that because of the magnetic field, the softer π^\pm and π^0 could be separated at the ECAL. Even if the two pions overlap in the ECAL, the π^0 momentum can be obtained by subtracting the track momentum from the total momentum measured in ECAL, assuming negligible contamination from other sources of energy deposition.

We also neglect the neutral pion combinatoric issue, which is justified if the respective parent rho mesons are boosted far apart as a result of the Higgs decay. In general, the π^\pm and π^0 coming from the same ρ^\pm parent are mostly collinear. This fact has been exploited in the hadronic tau tagging algorithm. For example, the HPS algorithm used by CMS requires that the charged and neutral hadrons are contained in a cone of the size $\Delta R = (2.8 \text{ GeV}/c)/p_T^{\tau h}$, where $p_T^{\tau h}$ is the transverse momentum of the reconstructed tau [26]. Since the two tau candidates are usually required to be well separated, the combinatorics problem in determining the correct ρ^\pm parents can be ignored.

A. Truth level

Recall from (23) and (37) that the minimum of the Θ distribution is located at 2Δ , and so constructing the Θ distribution allows us to read off the Δ phase of the underlying signal model. In figure 2, we show the Θ distribution in $pp \rightarrow hj$ events where we have temporarily assumed the neutrinos are fully reconstructed. The various signal models with $\Delta = 0$ (CP -even), $\Delta = \pi/4$ (maximal CP admixture), and $\Delta = \pi/2$ (CP -odd) clearly show the large $-\cos(\Theta - 2\Delta)$ contribution of the matrix element as seen in (37). We also superimpose the Θ distribution from $pp \rightarrow Zj$ event. Note that it is flat. Clearly, observing the cosine oscillation in experimental data will require both a favorable signal to background ratio as well as a solution for the neutrino momenta that preserves the inherently large amplitude of the Θ oscillation.

We now compare Θ at truth level with the ϕ^* variable proposed in Refs. [15, 16]: here, ϕ^* is the acoplanarity angle between the decay planes of ρ^+ and ρ^- in the $\rho^+\rho^-$ rest frame. The sign of ϕ^* is defined as the sign of the product of $\vec{p}_{\pi^-} \cdot (\vec{p}_{\pi^+} \times \vec{p}_{\pi^0})$. Following [15, 16], the events are divided into two classes, $y_+y_- < 0$ and $y_+y_- > 0$, where the two classes differ by a 180° phase shift. In order to make a direct comparison with our Θ variable, we combine the ϕ^* distributions of the two classes with a 180° phase shift so the phases of the two classes agree. Note that while ϕ^* does not refer to the neutrinos, this classification into the two classes still requires the knowledge of the neutrino momenta (see (21)). Assuming the neutrinos are fully reconstructed, the Θ and ϕ^* distributions for $pp \rightarrow hj$ events are shown in figure 3 with $\Delta = 0$. We readily see that oscillation amplitude of the Θ

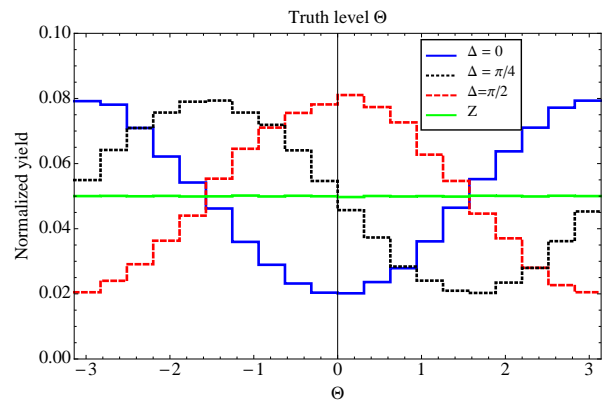


FIG. 2: The Θ distributions (compare with (37)) for the Higgs with $\Delta = 0$ (CP -even), $\Delta = \pi/4$ (maximal CP admixture), and $\Delta = \pi/2$ (CP -odd), and the Z , assuming neutrinos are fully reconstructed. The relative normalization of the Z line is arbitrary.

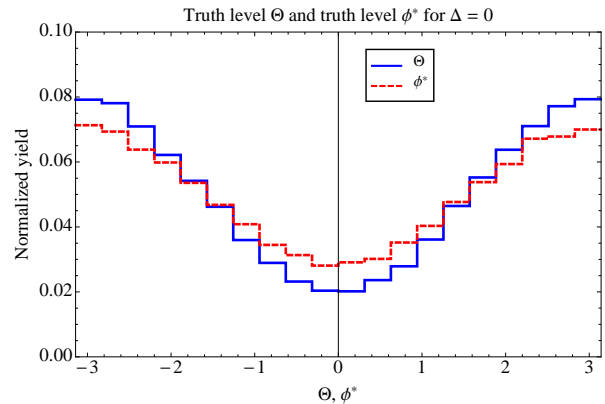


FIG. 3: The distributions of our Θ and the ϕ^* variable of Ref. [15, 16] for $\Delta = 0$. The ϕ^* distribution is aggregated from the two $y_+y_- > 0$ and $y_+y_- < 0$ classes as explained in the text to make the direct comparison clearer.

distribution is larger than that of the acoplanarity angle ϕ^* by about 50%. Compared to ϕ^* , the Θ variable thus provides superior sensitivity to the CP phase Δ .

Having considered the case where the neutrinos from the tau decays are fully reconstructed, we next turn to the lepton collider environment, where we will find the neutrinos can be fully reconstructed up to a two-fold ambiguity.

B. An e^+e^- Higgs Factory

At a lepton collider running at $\sqrt{s} = 250 \text{ GeV}$, such as the ILC, the main production mode for the Higgs is via associated production with a Z boson. Our prescribed decay mode for the Higgs, $h \rightarrow \pi^+ \pi^0 \bar{\nu} \pi^- \pi^0 \nu$, has two

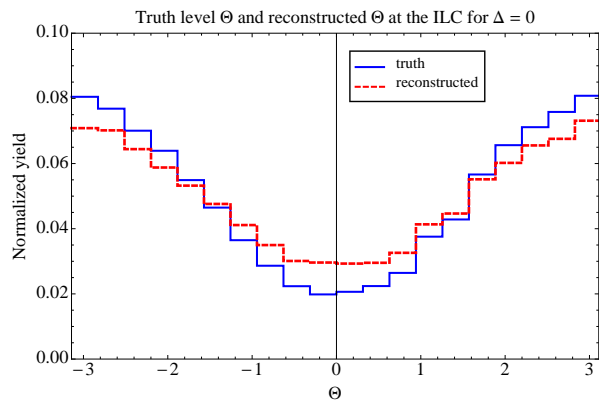


FIG. 4: The truth and reconstructed Θ distributions at the ILC for $\Delta = 0$.

neutrinos that escape the detector. We use the known initial four momenta, two tau mass and two neutrino mass constraints to solve for each neutrino momentum component. Note we will assume the Z decays to visible states, which will reduce our event yield by 20%. Solving the system of equations for the neutrino momenta gives rise to a two-fold ambiguity, where one solution is equal to the truth input neutrino momenta while the other gives a set of wrong neutrino momenta. Note both solutions are consistent with four-momentum conservation and therefore correctly reconstruct the Higgs mass. Since these solutions are indistinguishable in the analysis, we assign each solution half an event weight.

The resulting distribution of Θ for $\Delta = 0$ is given in figure 4, where we superimpose the truth level Θ distribution for $e^+e^- \rightarrow Zh$ events for easy comparison. We can see that the oscillation amplitude at the ILC is degraded from the truth level result by $\sim 30\%$. We also show the reconstructed distribution for $\Delta = 0$, $\Delta = \pi/4$, and $\Delta = \pi/2$ in figure 5. While the two-fold ambiguity for the neutrino momenta solution set does degrade the truth level result, the *reconstructable* Θ distribution in figure 5 shows significant discrimination power between various Δ signal models. Note the amplitude of pseudoscalar distribution ($\Delta = \pi/2$) is slightly higher than the scalar amplitude: here, the “wrong solution” approximates the correct neutrino momenta on average better than the other $\Delta = 0$ or $\Delta = \pi/4$ cases. This small effect can be traced back to equation (9) where we derived that a pseudoscalar decays to two taus in the singlet spin state. As a result, in this case the two tau spins point in opposite directions, regardless of the spin quantization axis. In the pseudoscalar case the two tau decays thus tend to occur with opposite orientation and the two neutrinos are slightly more back-to-back and consequently the two solutions for their momenta are closer together.

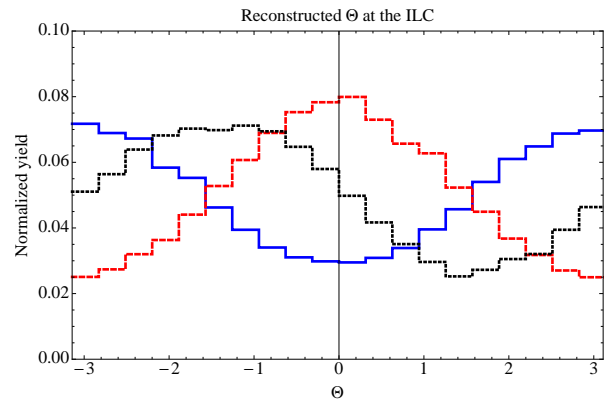


FIG. 5: The reconstructed Θ distribution at the ILC for $\Delta = 0$, $\Delta = \pi/4$, and $\Delta = \pi/2$.

$\sigma_{e^+e^- \rightarrow hZ}$	0.30 pb
$\text{Br}(h \rightarrow \tau^+\tau^-)$	6.1%
$\text{Br}(\tau^- \rightarrow \pi^-\pi^0\nu)$	26%
$\text{Br}(Z \rightarrow \text{visibles})$	80%
N_{events}	990
Accuracy	4.4°

TABLE I: Cross section, branching fractions, expected number of signal events, and accuracy for measuring Δ for the ILC with $\sqrt{s} = 250$ GeV and 1 ab^{-1} integrated luminosity.

We now discuss the projected ILC sensitivity for measuring Δ . At the ILC, the cross section for Zh production at $\sqrt{s} = 250$ GeV with polarized beams $P(e^-, e^+) = (-0.8, 0.3)$ for $m_h = 125$ GeV is 0.30 pb [27].⁶ Assuming a Higgs branching fraction to tau pairs of 6.1%, a $\tau^- \rightarrow \rho^-\nu \rightarrow \pi^-\pi^0\nu$ branching fraction of 26%, and a Z -to-visible branching fraction of 80%, we calculate the ILC should have 990 events with 1 ab^{-1} of luminosity. Since the solved neutrino momenta correctly reconstruct the Higgs mass, the ZZ backgrounds are negligible and will be ignored.

To estimate the expected ILC accuracy for measuring Δ , we perform a log likelihood ratio test for the SM hypothesis with $\Delta = 0$ against an alternative hypothesis with $\Delta = \delta$. In general, the likelihood ratio in N bins is given by

$$L = \frac{\prod_{i=1}^N \text{Pois}(B_i + S_i^{\Delta=0} | B_i + S_i^{\Delta=\delta})}{\prod_{i=1}^N \text{Pois}(B_i + S_i^{\Delta=0} | B_i + S_i^{\Delta=0})}, \quad (38)$$

where B_i , $S_i^{\Delta=0}$ and $S_i^{\Delta=\delta}$ are the number of background events, signal events assuming $\Delta = 0$, and sig-

⁶ We have checked the Θ distribution is insensitive to the polarization of the e^-e^+ beams.

nal events assuming $\Delta = \delta$ in bin i of the Θ distribution. In our ILC treatment, we neglect ZZ and $Z \rightarrow \tau\tau$ continuum backgrounds and so we set $B_i = 0$. Here, $\text{Pois}(k|\lambda)$ is the usual Poisson distribution function, $\text{Pois}(k|\lambda) = \lambda^k e^{-\lambda}/k!$.

We parametrize the signal Θ distribution with a $c - A \cos(\Theta - 2\Delta)$ fit function, where the offset constant c and oscillation amplitude A are fixed by the fit of the standard model Θ distribution with $\Delta = 0$, giving c_0 and A_0 respectively. Then, the resulting $S^{\Delta=\delta}$ signal Θ distribution is given by $c_0 - A_0 \cos(\Theta - 2\delta)$. We construct the binned likelihood⁷ according to (38) for various δ hypotheses to test the discrimination against the SM hypothesis. With 1 ab^{-1} of ILC luminosity, we find 1σ discrimination at $\delta = 0.077 \text{ rad} = 4.4^\circ$, which is a highly promising degree of sensitivity for measuring the CP phase of the Higgs coupling to taus. We summarize our rate estimate and accuracy result in table I.

We remark that this sensitivity estimate is only driven by statistical uncertainties, and systematic uncertainties are expected to reduce the efficacy of our result. Also, detector resolution effects and SM backgrounds, while expected to be small, will also slightly degrade our projection. Based on our results, which surpass earlier accuracy estimates of 6° [18], a full experimental sensitivity study incorporating these subleading effects is certainly warranted.

C. LHC

We now develop an LHC study for reconstructing the Θ distribution in $pp \rightarrow hj$ in the $\pi^+\pi^0\pi^-\pi^0 + j + \cancel{E}_T$ final state. We use the $h + j$ final state for a couple of reasons. First, since hadronic taus can be faked by jets, $pp \rightarrow h \rightarrow$ two hadronic taus faces an immense background from multijet QCD. By requiring another object in the final state, we gain handles to suppress the background. Second, the collinear approximation gives ambiguous results if the two taus are back-to-back, so the requirement of an additional object in the event guarantees we are away from this configuration. One option is associated production of a Higgs with a W/Z . However this rate is quite small, especially once the branching ratios for W/Z into clean final states are taken into account. Other possibilities include Higgs production via vector boson fusion and in association with a jet. Both of these options give promising signal-to-background ratios and both should be considered. For concreteness we will consider $pp \rightarrow h + j$ here as a demonstration of the feasibility of our technique.

As mentioned before, the neutrinos are not reconstructible in the hadron collider environment, and so we

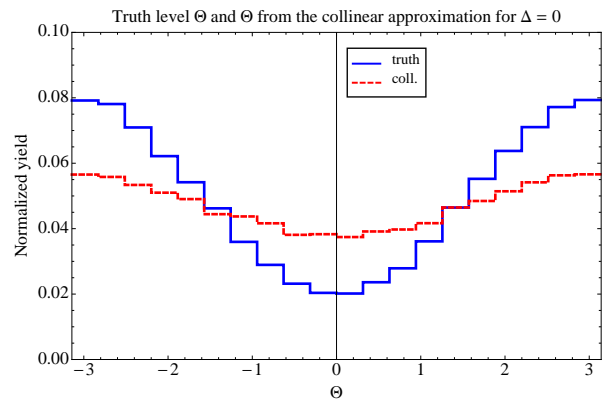


FIG. 6: The distributions of the truth- Θ and Θ from the collinear approximation for $\Delta = 0$.

will employ the collinear approximation [23] for the neutrino momenta. In figure 6, we show a comparison between the truth level Θ distribution and the Θ distribution using the collinear approximation for neutrino momenta, for the $\Delta = 0$ benchmark. While the collinear approximation reduces the oscillation amplitude of the distribution, the location of the minimum of the distribution does not change. Therefore, measuring Δ is a viable possibility at the LHC using the collinear approximation for the neutrino momenta. We remark that in the collinear approximation, Θ is equivalent to the acoplanarity angle ϕ^* [15, 16]. Yet, we are the first feasibility study for measuring CP violation in the Higgs coupling to taus at hadron colliders using prompt tau decays and kinematics. With a more sophisticated scheme than the collinear approximation, the Θ variable will be superior to ϕ^* .

At the LHC, the dominant background for the hj signal process is the irreducible Zj background, where the Z decays to the same final state as the higgs. As shown earlier in figure 2, the Θ distribution from Z events is flat: importantly, this is true regardless of possible mass window cuts on the reconstructed $m_{\tau\tau}$ resonance. We remark that the CP phase in the Higgs coupling to taus does manifest in the $Z-\tau-\tau$ vertex at one loop. Since this effect is suppressed by $\sim y_\tau^2/(16\pi^2) \sim \mathcal{O}(10^{-4})$, whereas the signal to background ratio will be $\mathcal{O}(60\%)$, we can safely ignore the loop induced CP phase in the $Z-\tau-\tau$ vertex. In addition, we will assume that the QCD background contribution also has a flat Θ distribution, since the QCD contamination in the signal region is not expected to have any particular spin correlations.

Using our hj and Zj event samples from MadGraph 5 for a 14 TeV LHC, we first isolate the signal region with a series of hard cuts. First, we apply a preselection requirement on the leading jet $p_T > 140 \text{ GeV}$ with $|\eta| < 2.5$. Using MCFM v.6.6 [28] with these preselection requirements on the leading jet, we obtain a hj NLO inclusive

⁷ We choose $N = 100$ bins, though we verified the number of bins is immaterial for our results.

	$h j$	$Z j$
Inclusive σ	2.0 pb	420 pb
$\text{Br}(\tau^+\tau^- \text{ decay})$	6.1%	3.4%
$\text{Br}(\tau^- \rightarrow \pi^-\pi^0\nu)$	26%	26%
Cut efficiency	18%	0.24%
N_{events}	1100	1800

TABLE II: Cross sections, branching fractions, cut efficiencies, and expected number of events assuming 3 ab^{-1} and 50% τ tagging efficiency for the Higgs signal and the Z background: the background number of events includes an additional 10% contribution from QCD multijet background.

cross section of 2.0 pb with $m_h = 126 \text{ GeV}$ and a $Z j$ NLO inclusive cross section of 420 pb. After applying the appropriate Higgs, Z , and tau branching fractions, we calculate a signal cross section of 8.2 fb and Z background cross section of 970 fb.⁸ Next, we impose hard kinematic cuts to isolate the signal. Motivated by [11], we choose the signal region to be:

- $\cancel{E}_T > 40 \text{ GeV}$,
- $p_T^{\rho^\pm} > 45 \text{ GeV}$,
- $|\eta^{\rho^\pm}| < 2.1$,
- $m_{\text{coll}} > 120 \text{ GeV}$,

where m_{coll} is the reconstructed Higgs mass by using the collinear approximation. The hard m_{coll} cut strongly suppresses the $Z + j$ background, but is less effective on multijet QCD. To reduce the multijet component – and its accompanying uncertainty – to less than 10% of the total background we impose a high \cancel{E}_T cut. The net efficiencies for signal and Z background after these cuts are 18% and 0.24%, respectively. Rather than simulate the QCD contribution, we account for QCD contamination in the signal region by increasing the Z background rate by 10%: a complete treatment of the expected QCD background is beyond the scope of this study. Finally, for hadronic τ tagging efficiency, we consider a standard 50% efficiency and a more optimistic 70% efficiency [26]. We therefore expect 1100 signal events and 1800 $Z + \text{QCD}$ background events with 3 ab^{-1} of luminosity from the 14 TeV LHC, assuming 50% τ tagging efficiency. These rates are summarized in table II.

We note that although we generated signal and background samples independently, there is a small interference between Higgs and Z diagrams in the $gq \rightarrow \tau^+\tau^-q$

τ_h efficiency	50%	70%
3σ	$L = 550 \text{ fb}^{-1}$	$L = 300 \text{ fb}^{-1}$
5σ	$L = 1500 \text{ fb}^{-1}$	$L = 700 \text{ fb}^{-1}$
Accuracy($L = 3 \text{ ab}^{-1}$)	11.5°	8.0°

TABLE III: The luminosity required for distinguishing the scalar and pseudoscalar couplings and the accuracy in measuring Δ with 3 ab^{-1} of luminosity at the 14 TeV LHC.

diagram. Our checks of this interference on the Θ distributions for combined signal and background events versus separate signal and background events showed a negligible effect: we thus ignore this interference effect.

We now perform a likelihood analysis (38) to quantify how effectively the Θ distribution distinguishes between signal hypotheses with different CP phases in the presence of $Z + \text{QCD}$ background. First, we test the discrimination between a pure scalar and a pure pseudoscalar $h\text{-}\tau\text{-}\tau$ coupling. We find that these two hypotheses can be distinguished at 3σ sensitivity with 550 (300) fb^{-1} assuming 50% (70%) τ tagging efficiency. We can attain 5σ sensitivity between pure scalar and pseudoscalar couplings with 1500 (700) fb^{-1} luminosity assuming 50% (70%) efficiency.

We also estimate the possible accuracy for the LHC experiments to measure Δ with an upgraded luminosity of 3 ab^{-1} . We adopt the same procedure as with the ILC accuracy estimate described in the previous section, modified to account for the $Z + \text{QCD}$ background, which is fixed to be flat in Θ . We find that the accuracy in measuring Δ is 11.5° (8.0°) assuming 50% (70%) hadronic τ tagging efficiency. The scalar versus pseudoscalar discrimination and the accuracy estimates are summarized in table III.

Again, these estimates are based only on statistical uncertainties without performing a full detector simulation. The effects from pileup and detector resolution are expected to degrade these projections, but corresponding improvements in the analysis, such as a more precise approximation for the neutrino momenta, improved background understanding (from other LHC measurements) or multivariate techniques, could counterbalance the decrease in sensitivity. The promising results of our study strongly motivate a comprehensive analysis by the LHC experiments for the prospect of measuring the CP phase Δ .

V. CONCLUSIONS

Higgs decays to tau leptons provide a singular opportunity to measure the CP properties of the Higgs-fermion couplings. In this paper, we have studied the decay of $h \rightarrow \tau^+\tau^-$ followed by $\tau^\pm \rightarrow (\rho^\pm \rightarrow \pi^\pm\pi^0)\nu$. A new observable, Θ , was constructed in (36) using the momenta of the tau decay products. The differential cross section

⁸ These numbers were generated using CTEQ6M parton distribution functions. For the signal we use a factorization/renormalization scale of $\mu_F = m_H/2$, while for the background we use $\mu_F = \sqrt{M_Z^2 + p_{T,j}^2}$. These scale choices are motivated by agreement with higher order (NNLO) calculations (where they exist).

can be written in a form of $c - A \cos(\Theta - 2\Delta)$, hence the Θ distribution can be used to distinguish various CP mixing as shown in figure 2. The Θ variable can be viewed as an acoplanarity angle between the planes spanned by certain linear combinations of the pion and neutrino momenta, and it was demonstrated to be superior to previously proposed acoplanarity angles.

At the ILC, where the neutrino momenta can be reconstructed up to a two-fold ambiguity, the advantages of the Θ variable are most evident. We estimate that the CP phase can be measured to an accuracy of 4.4° for $\sqrt{s} = 250$ GeV, a substantial improvement over previous results. For the LHC, we have had to rely on the collinear approximation to reconstruct the neutrino momenta and some of the discriminating power of the Θ variable is lost. Nevertheless, we find an accuracy of 11.5° (8.0°) is possible after 3000 fb^{-1} of luminosity and assuming a 50% (70%) tau tagging efficiency. Recasting in terms of the parameters introduced in (3), a 5° – 10° deviation from the SM case is equivalent to sensitivity to $\Lambda \sim 10$ TeV, where Λ is the scale of the dimension six operator in (3) and $|\beta|$ is assumed to be $\mathcal{O}(1)$. A better approximation scheme for the neutrino momenta will improve these results.

In our collider studies we have neglected detector effects and background systematic uncertainties. While adding these effects will worsen our results, this may be offset by better understanding of the backgrounds (thereby allowing looser cuts) and with a more sophisticated (*e.g.* MVA) analysis and statistical tools.

Finally, in this work we picked specific Higgs production mechanisms and focused on a single decay channel. To understand the full extent of future colliders' sensitivities to the CP phase of Higgs-fermion couplings, additional production channels such as VBF should be explored, both at the LHC and in a Higgs factory. In addition, other hadronic decay channels, as well as semi-leptonic channels, of the tau pair might also be sensitive to the CP properties of the Higgs.

Acknowledgments

We would like to thank Kaustubh Agashe, Wolfgang Altmannshofer, Yuval Grossman, Uli Haisch, Josh Ruderman, Daniel Stolarski, Raman Sundrum, Ciaran Williams and Jure Zupan for comments and discussions. We would also like to thank the Kavli Institute for Theoretical Physics at UCSB where part of this work was performed. RP is supported by the NSF under grant PHY-0910467. TO is supported by the DOE under grant DE-FG02-13ER41942. Fermilab is operated by the Fermi Research Alliance, LLC under Contract No. De-AC02-07CH11359 with the United States Department of Energy.

Appendix A: A Simple UV Completion of the Dimension-6 Operator

In this appendix we give an example for a UV completion for the dimension-6 operator in (3), *i.e.*, the term with β . Our purpose is not to advocate a specific model as particularly well-motivated but to simply provide an existence proof of a weakly-coupled renormalizable theory that can generate the β term in (3) at $\Lambda \sim 1$ TeV with an arbitrary CP phase, without generating other operators that may contradict with experiments.

Consider an extension of the SM with a second higgs doublet Φ with $m_\Phi \gtrsim 1$ TeV with the following tree-level lagrangian:

$$\begin{aligned} \mathcal{L}_{\text{tree}} = & \mathcal{L}_{\text{SM}-y_\tau} \\ & + |\text{D}\Phi|^2 - m_\Phi^2 |\Phi|^2 - \lambda_\Phi |\Phi|^4 \\ & - (yH\ell_{3L}^\dagger \tau_R + y'\Phi\ell_{3L}^\dagger \tau_R + \lambda'(\Phi^\dagger H)|H|^2 + \text{c.c.}), \end{aligned} \quad (\text{A1})$$

where $\mathcal{L}_{\text{SM}-y_\tau}$ is the SM lagrangian without the tau Yukawa coupling. The full quantum lagrangian is $\mathcal{L}_{\text{tree}} + \mathcal{L}_{\text{ct}}$, where \mathcal{L}_{ct} contains all counterterms *necessary* for consistent renormalization at loop level. For simplicity, we neglect neutrino masses and mixings, so $\mathcal{L}_{\text{tree}}$ possesses an accidental $U(1)_e \times U(1)_\mu \times U(1)_\tau$ family symmetry, which is then inherited by \mathcal{L}_{ct} as well. This immediately implies that there are no lepton flavor changing processes such as $\mu \rightarrow e\gamma$. There are no constraints from quark flavor/ CP measurements; since the couplings of Φ to quarks are absent in $\mathcal{L}_{\text{tree}}$ and only appear in \mathcal{L}_{ct} , they are not only very small ($\sim y'/16\pi^2 \times$ the corresponding SM Yukawa) but also respect the CKM flavor structure of the SM. Similarly, the couplings of Φ to e and μ are inconsequential; in particular, we have checked that a contribution to the electron electric dipole moment induced at 2-loop level is negligible. Finally, the modification of the coupling of Z to τ is also tiny, safely below the LEP constraints.

In order to see the effects of (A1) on Higgs decays let us consider the limit in which $m_\Phi \gg v$ and the doublet Φ can be integrated out and we can consider an effective field theory below m_Φ . At tree level, this generates two dimension-6 interactions:

$$\mathcal{L}_{\text{dim-6}} = \frac{|\lambda'|^2}{m_\Phi^2} |H|^6 + \left(\frac{\lambda' y'}{m_\Phi^2} |H|^2 H \ell_{3L}^\dagger \tau_R + \text{c.c.} \right). \quad (\text{A2})$$

This theory now matches on to the effective theory (3) with $\alpha = y$, $\beta = y'\lambda'$ and $\Lambda = m_\Phi$. It should be noted that this theory contains in general a CP violating phase. In particular, the phase of $y^* y' \lambda'$ may not be rotated away by field redefinitions. Taking $\Lambda \sim \text{TeV}$ and $|\lambda'| \sim |y'| \sim 1$ with arbitrary phases in y , y' and λ' can therefore produce an $\mathcal{O}(1)$ CP -violating phase in Higgs decays to tau leptons.

Other theories, including composite Higgs models [29, 30] and models with vector-like leptons [31] may also produce the necessary interactions to induce CP violating

Higgs decays into taus. In constructing such models one should take care that the coupling of Z to taus is not modified above the 10^{-3} level (see Ref. [32] or Fig. 10.4

of [33]) either by construction (as in the model we just discussed) or by a cancellation among various contributions.

-
- [1] G. Aad *et al.* [ATLAS Collaboration], Phys. Lett. B **716**, 1 (2012) [arXiv:1207.7214 [hep-ex]].
- [2] S. Chatrchyan *et al.* [CMS Collaboration], Phys. Lett. B **716**, 30 (2012) [arXiv:1207.7235 [hep-ex]].
- [3] [ATLAS Collaboration], ATLAS-CONF-2013-034. [CMS Collaboration], CMS-PAS-HIG-13-005.
- [4] T. Aaltonen *et al.* [CDF and D0 Collaborations], arXiv:1303.6346 [hep-ex].
- [5] S. Chatrchyan *et al.* [CMS Collaboration], Phys. Rev. Lett. **110**, 081803 (2013) [arXiv:1212.6639 [hep-ex]].
- [6] [ATLAS Collaboration], ATLAS-CONF-2013-013.
- [7] S. Bolognesi, Y. Gao, A. V. Gritsan, K. Melnikov, M. Schulze, N. V. Tran and A. Whitbeck, Phys. Rev. D **86**, 095031 (2012) [arXiv:1208.4018 [hep-ph]].
- [8] Y. Grossman and I. Nachshon, JHEP **0807**, 016 (2008) [arXiv:0803.1787 [hep-ph]].
- [9] F. Bishara, Y. Grossman, R. Harnik, D. Robinson, J. Shu and J. Zupan, in progress.
- [10] R. Primulando, D. Stolarski and J. Zupan, in progress.
- [11] [CMS Collaboration], CMS-PAS-HIG-13-004.
- [12] J. R. Dell'Aquila and C. A. Nelson, Nucl. Phys. B **320**, 86 (1989).
- [13] J. R. Dell'Aquila and C. A. Nelson, Nucl. Phys. B **320** (1989) 61.
- [14] B. Grzadkowski and J. F. Gunion, Phys. Lett. B **350**, 218 (1995) [hep-ph/9501339].
- [15] G. R. Bower, T. Pierzchala, Z. Was and M. Worek, Phys. Lett. B **543**, 227 (2002) [hep-ph/0204292].
- [16] M. Worek, Acta Phys. Polon. B **34**, 4549 (2003) [hep-ph/0305082].
- [17] K. Desch, Z. Was and M. Worek, Eur. Phys. J. C **29**, 491 (2003) [hep-ph/0302046].
- [18] K. Desch, A. Imhof, Z. Was and M. Worek, Phys. Lett. B **579**, 157 (2004) [hep-ph/0307331].
- [19] S. Berge and W. Bernreuther, Phys. Lett. B **671**, 470 (2009) [arXiv:0812.1910 [hep-ph]].
- [20] S. Berge, W. Bernreuther and J. Ziethe, Phys. Rev. Lett. **100**, 171605 (2008) [arXiv:0801.2297 [hep-ph]].
- [21] S. Berge, W. Bernreuther, B. Niepelt and H. Spiesberger, Phys. Rev. D **84**, 116003 (2011) [arXiv:1108.0670 [hep-ph]].
- [22] S. Berge, W. Bernreuther and H. Spiesberger, arXiv:1208.1507 [hep-ph].
- [23] R. K. Ellis, I. Hinchliffe, M. Soldate and J. J. van der Bij, Nucl. Phys. B **297**, 221 (1988).
- [24] N. D. Christensen and C. Duhr, Comput. Phys. Commun. **180**, 1614 (2009) [arXiv:0806.4194 [hep-ph]].
- [25] J. Alwall, M. Herquet, F. Maltoni, O. Mattelaer and T. Stelzer, JHEP **1106** (2011) 128 [arXiv:1106.0522 [hep-ph]].
- [26] C. Collaboration *et al.* [CMS Collaboration], JINST **7**, P01001 (2012) [arXiv:1109.6034 [physics.ins-det]].
- [27] ILC Technical Design Report, Vol. 2, [ILC Collaboration] <http://www.linearcollider.org/ILC/TDR>
- [28] J. M. Campbell, R. K. Ellis and C. Williams, JHEP **1107**, 018 (2011) [arXiv:1105.0020 [hep-ph]].
- [29] K. Agashe, R. Contino and A. Pomarol, Nucl. Phys. B **719**, 165 (2005) [hep-ph/0412089].
- [30] G. F. Giudice, C. Grojean, A. Pomarol and R. Rattazzi, JHEP **0706** (2007) 045 [hep-ph/0703164].
- [31] J. Kearney, A. Pierce and N. Weiner, Phys. Rev. D **86**, 113005 (2012) [arXiv:1207.7062 [hep-ph]].
- [32] S. Schael *et al.* [ALEPH and DELPHI and L3 and OPAL and SLD and LEP Electroweak Working Group and SLD Electroweak Group and SLD Heavy Flavour Group Collaborations], Phys. Rept. **427**, 257 (2006) [hep-ex/0509008].
- [33] J. Beringer *et al.* [Particle Data Group Collaboration], Phys. Rev. D **86**, 010001 (2012).